

## Analysis and Control of a Capsubot

Y. Liu\*, H. Yu\*, and T. C. Yang\*\*

\*Faculty of Computing, Engineering and Technology, Staffordshire University, Stafford, UK  
(e-mail: {y.liu, h.yu} @ staffs.ac.uk)

\*\* School of Engineering and Information Technology, Sussex University, Brighton, UK

**Abstract:** In this paper, a special underactuated system – a capsule robot, also called capsuobot, is studied to investigate the tracking control issue of underactuated dynamic systems. A seven-step motion strategy of the capsuobot is proposed. A trajectory profile is designed based on the proposed motion strategy. By using this profile, the capsuobot can move effectively in a desired direction. Three control approaches are investigated: an open-loop control approach, a closed-loop control approach using partial feedback linearization technique, and a simple switch control approach. Extensive simulation studies are conducted to demonstrate the proposed approaches.

### 1. INTRODUCTION

In recent years, the capsule robot (capsuobot) has attracted great attention from researchers due to its extensive potential applications in medical treatment, engineering diagnosis, and disaster rescue, etc. The capsuobot is a kind of autonomous micro mobile robot which can explore fields inaccessible to humans and send back useful data for analysis. In general, there are two types of capsuobot. One is the legged capsuobot which has an external driving mechanism outside the capsule (Karagozler *et al.* (2006)) (Kosa *et al.* (2005)). The disadvantage of this type of capsuobot is that the complex structure of its mechanism makes it difficult to control in rigorous environments (Stefanini *et al.* (2006)). The other main type is the legless capsuobot which is driven by internal impact force and friction (Li *et al.* (2006)) (Kim *et al.* (2005)). This type of capsuobot has a simple driving structure and can be positioned precisely in a complicated environment. However, stability and tracking performance are significant factors for an autonomous robot. Most current research on the legless capsuobot focuses on the design of capsule structure and the method of driving, while the modelling, optimization and control of capsuobots have been neglected.

This paper investigates a legless capsuobot from the viewpoint of underactuated dynamic systems, which have fewer independent control actuators than degrees of freedom to be controlled. The structure of the mechanism is derived from Yamagata and Higuchi (1995) who move an object under friction using impulsive propulsion, utilizing the reactive theory between two different weight objects. The object can move along a straight line by applying periodic propulsion. Chernousko (2002) has investigated this mechanism from the aspect of physics. In (Chernousko (2002)), the optimum parameters of the system and a control law have been proposed. Using the same philosophy, a special underactuated system – the pendulum-driven cart-pole system – has been proposed (Li *et al.* (2005)). The trajectory tracking problem of the pendulum-driven cart-pole system was later investigated by Liu *et al.* (2007) and the system tracking problem studied using control concepts. A motion

strategy-based trajectory profile has been studied, and an open-loop control law has been proposed. In (Yu *et al.* (2007)), a closed-loop control law has been investigated on the pendulum-driven cart-pole system. In this paper, we will use the same idea to study a trajectory tracking problem on a capsuobot. The purpose of this paper is to drive the capsuobot in a desired direction. Based on the reactive theory, a seven-step motion strategy is proposed. Two trajectory tracking-based control approaches which are the open-loop control (OLC) approach and the closed-loop control (CLC) approach are studied. Further, a simple switch control (SSC) approach is proposed for controlling the capsuobot. The SSC approach which utilizes the control experience of other two approaches can easily be implemented in a real experimental rig, and is robust to external disturbance.

This paper is structured as follows. In section 2, the dynamic model of the capsuobot is given. In section 3, a seven-step motion strategy and the formula of the trajectory profile are studied. In section 4, an optimum selection of the desired trajectory profile is proposed. Three control approaches are studied in section 5. In section 6, extensive simulation studies are presented and a comparison made between them. Finally, concluding remarks are made, and future work are discussed.

### 2. DYNAMIC MODELLING OF THE CAPSUBOT

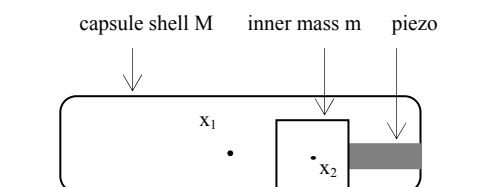


Figure 1 Capsuobot System

The capsuobot researched in this paper is shown in Figure 1. The system consists of three elements: the capsule shell, a piezoelectric element and an inner mass. The propulsion force is generated by the piezoelectric element which acts between the capsule shell and the inner mass.  $M$  is the mass of the capsule shell,  $m$  is the inner mass,  $u$  is the propulsion force between the shell and the inner mass,  $g$  is acceleration due to gravity. Consider the shell center and the inner mass

center as reference points;  $x_1$  is the position of the capsule shell, and  $x_2$  is the position of the inner mass. In order to distinguish the static friction and the kinetic friction between the shell and the ground, we use  $\mu_{1s}$  as the static friction coefficient, and  $\mu_{1k}$  as the kinetic friction coefficient between the capsule shell and the environment.  $\mu_{2s}$  is the static friction coefficient and  $\mu_{2k}$  is the kinetic friction coefficient between the inner mass and the capsbot.

Let the capsule shell center be the origin of the coordinate. Using Newton's second law, during the fast motion the following two relations can be found

$$M\ddot{x}_1 + \mu_{1k}(M+m)g \operatorname{sgn}(\dot{x}_1) - \mu_{2k}mg \operatorname{sgn}(\dot{x}_2 - \dot{x}_1) = u \quad (1)$$

$$m\ddot{x}_2 + \mu_{2k}mg \operatorname{sgn}(\dot{x}_2 - \dot{x}_1) = -u \quad (2)$$

Putting (2) in (1) and rewriting (1) give

$$M\ddot{x}_1 + m\ddot{x}_2 + \mu_{1k}(M+m)g \operatorname{sgn}(\dot{x}_1) = 0 \quad (3)$$

Let  $q_1=x_1$  and  $q_2=x_2$ . Equations (2) and (3) can be written in a general compact form

$$\begin{cases} D_{11}\ddot{q}_1 + D_{12}\ddot{q}_2 + h_1(q_1, \dot{q}_1, q_2, \dot{q}_2) = 0 \\ D_{21}\ddot{q}_1 + D_{22}\ddot{q}_2 + h_2(q_1, \dot{q}_1, q_2, \dot{q}_2) = \tau \end{cases} \quad (4)$$

where  $D_{11}=M$ ,  $D_{12}=m$ ,  $D_{21}=0$ ,  $D_{22}=m$ ,

$h_1 = \mu_{1k}(M+m)g \operatorname{sgn}(\dot{x}_1)$ ,  $h_2 = \mu_{2k}mg \operatorname{sgn}(\dot{x}_2 - \dot{x}_1)$ ,  $\tau = -u$ .

It is typical of an underactuated system that the capsbot has one control input generated by the piezoelectric element, while two variables, the capsule shell position and the inner mass position, have to be controlled.

### 3. MOTION GENERATION ANALYSIS

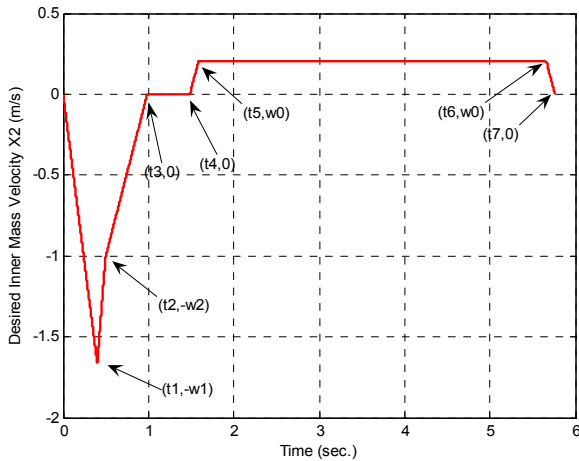


Figure 2 Desired inner mass velocity profile for one cycle

To move the capsule shell in one direction, the motion needs to be considered in two stages: 1) Fast motion stage: moving the inner mass fast using  $|u| \gg \mu_{1s}(M+m)g + \mu_{2k}mg$ ; 2) Slow motion stage: moving the inner mass slowly to its initial position using  $|u| < \mu_{1s}(M+m)g - \mu_{2k}mg$ . By using these constraints, a desired inner mass velocity profile can be generated as shown in Figure 2. A detailed description of the

seven steps of the procedure corresponding to the diagram is presented below.

- 1)  $t \in [0, t_1]$ : Fast backward accelerated motion of  $m$  ( $\ddot{x}_2 \ll 0$ ,  $\dot{x}_2 < 0$ ) leads to forward accelerated motion of  $M$  ( $\ddot{x}_1 > 0$ ,  $\dot{x}_1 > 0$ ).
- 2)  $t \in [t_1, t_2]$ : Fast backward decelerated motion of  $m$  ( $\ddot{x}_2 \gg 0$ ,  $\dot{x}_2 < 0$ ) leads to forward decelerated motion of  $M$  ( $\ddot{x}_1 < 0$ ,  $\dot{x}_1 > 0$ ).
- 3)  $t \in [t_2, t_3]$ : Small backward decelerated motion of  $m$  ( $0 < \ddot{x}_2 \leq \varepsilon_m$ ,  $\dot{x}_2 < 0$ ) and  $M$  remains stationary ( $\ddot{x}_1 = 0$ ,  $\dot{x}_1 = 0$ ).
- 4)  $t \in [t_3, t_4]$ :  $m$  ( $\ddot{x}_2 = 0$ ,  $\dot{x}_2 = 0$ ) and  $M$  remain stationary ( $\ddot{x}_1 = 0$ ,  $\dot{x}_1 = 0$ ).
- 5)  $t \in [t_4, t_5]$ : Small forward accelerated motion of  $m$  ( $0 < \ddot{x}_2 \leq \varepsilon_m$ ,  $\dot{x}_2 > 0$ ) and  $M$  remains stationary ( $\ddot{x}_1 = 0$ ,  $\dot{x}_1 = 0$ ).
- 6)  $t \in [t_5, t_6]$ : Uniform motion of  $m$  with a small velocity ( $\ddot{x}_2 = 0$ ,  $\dot{x}_2 = w_0$ ) and  $M$  remains stationary ( $\ddot{x}_1 = 0$ ,  $\dot{x}_1 = 0$ ).
- 7)  $t \in [t_6, t_7]$ : Small forward decelerated motion of  $m$  ( $-\varepsilon_m \leq \ddot{x}_2 < 0$ ,  $\dot{x}_2 > 0$ ) and  $M$  remains stationary ( $\ddot{x}_1 = 0$ ,  $\dot{x}_1 = 0$ ).

where  $\varepsilon_m$  is the maximal acceleration of the inner mass which keeps the capsule shell stationary. The cycle time is  $T=t_7$ . According to the division of the motion into two stages, steps 1 and 2 above are the fast motion stage, while the rest of the steps (steps 3-7) are the slow motion stage. The formula of the desired inner mass velocity  $\dot{x}_{2d}$  is given in (5).

$$\dot{x}_{2d}(t) = \begin{cases} -tw_1/t_1 & t \in [0, t_1) \\ -w_1 + (w_1 - w_2)(t - t_1)/(t_2 - t_1) & t \in [t_1, t_2) \\ w_2(t - t_3)/(t_3 - t_2) & t \in [t_2, t_3) \\ 0 & t \in [t_3, t_4) \\ w_0(t - t_4)/(t_5 - t_4) & t \in [t_4, t_5) \\ w_0 & t \in [t_5, t_6) \\ w_0(t_7 - t)/(t_7 - t_6) & t \in [t_6, t_7] \end{cases} \quad (5)$$

The parameters  $w_1$ ,  $w_2$ ,  $w_0$ , and  $t_1 \sim t_7$  have a significant effect on system performance. The optimum selection of these parameters will be discussed in section 4.

### 4. OPTIMUM SELECTION OF THE DESIRED VELOCITY PROFILE

To optimize the specific parameters in the profile, the following boundary conditions are assumed

$$\dot{x}_1(0) = \dot{x}_2(0) = 0, x_1(0) = 0, x_2(0) = a, \dot{x}_1(t_2) = 0, x_2(t_2) - x_1(t_2) = -a$$

where  $a$  is the initial position of the inner mass  $m$ .

**$t_1$  and  $w_1$ :** To find an efficient driving force in step 1, the energy usage per unit displacement is given as

$$\eta = \int_0^{t_1} u^2 dt / x_1(t_1) \quad (6)$$

Integrating (3) twice between  $[0, t_1]$ , gives

$$Mx_1(t_1) + \mu_{1k}(M+m)gt_1^2/2 + mx_2(t_1) - ma = 0$$

From the diagram of the desired profile, it gives

$$x_2(t_1) = a + \varepsilon_1 t_1^2 / 2$$

where  $\varepsilon_1$  is the acceleration in step 1). Thus, we have

$$x_1(t_1) = -[\mu_{1k}(M+m)g + m\varepsilon_1]t_1^2 / (2M) \quad (7)$$

Putting (2) and (7) in (6) gives

$$\eta = -\frac{2M(m\varepsilon_1 - \mu_{2k}mg)^2}{[\mu_{1k}(M+m)g + m\varepsilon_1]t_1}$$

Using  $d\eta/d\varepsilon_1 = 0$ , the efficient  $\varepsilon_1$  can be given as

$$\varepsilon_1 = -[2\mu_{1k}(M+m)g + \mu_{2k}mg] / m \quad (8)$$

From (8), efficient acceleration has no relation to the time duration of step 1. If the duration time  $t_1$  is given, we have

$$w_1 = [2\mu_{1k}(M+m)g + \mu_{2k}mg]t_1 / m \quad (9)$$

To choose a reasonable  $t_1$ , we can refer to (Liu *et al.* (2007)) and (Yu *et al.* (2007)).

**$t_2$  and  $w_2$ :** Integrating (3) once between  $[0, t_2]$ , using the boundary condition,  $w_2$  is given as

$$w_2 = -\dot{x}_2(t_2) = \mu_{1k}(M+m)gt_2 / m \quad (10)$$

Integrating (3) twice between  $[0, t_2]$ , the inner mass position at  $t_2$  is given

$$Mx_1(t_2) + \mu_{1k}(M+m)gt_2^2 / 2 + mx_2(t_2) - ma = 0$$

Using the boundary  $x_2(t_2) - x_1(t_2) = -a$ , we have

$$x_2(t_2) = (m-M)a / (M+m) - \mu_{1k}gt_2^2 / 2 \quad (11)$$

Another relation can be found using the diagram of the profile in Fig. 2 which is

$$x_2(t_2) = a + \varepsilon_1 t_1^2 / 2 - (w_1 + w_2)(t_2 - t_1) / 2 \quad (12)$$

Combining (11) and (12), we have

$$t_2 = (-b_2 + \sqrt{b_2^2 - 4b_1b_3}) / 2b_1 \quad (13)$$

and

$$w_2 = \mu_{1k}(-b_2 + \sqrt{b_2^2 - 4b_1b_3})(M+m)g / 2mb_1 \quad (14)$$

where  $b_1 = \mu_{1k}Mg/m$ ,  $b_2 = w_1 - \mu_{1k}(M+m)gt_1/m$ ,

$$b_3 = -4Ma/(M+m) - w_1t_1 - \varepsilon_1t_1^2$$

**$t_3$ :** In order to stop the inner mass fast while the capsule shell remains at rest in step 3, the maximal acceleration is used

$$\varepsilon_m = \mu_{1k}(M+m)g / m \quad (15)$$

So the duration of step 3 is given as

$$t_3 = t_2 + w_2 / \varepsilon_m \quad (16)$$

**$t_4$ :** Step 4 is crucial to stabilizing the system. It is the motion stage that both masses are at rest. The purpose of step 4 is to minimize the tracking errors caused by calculation and external disturbance. So,  $t_4$  can be properly selected according to system conditions.

**$t_5$  and  $w_0$ :** If  $t_5 - t_4$  is selected as a short duration,  $w_0$  will be obtained using the maximal acceleration

$$w_0 = \varepsilon_m(t_5 - t_4) = \mu_{1k}(M+m)g(t_5 - t_4) / m \quad (17)$$

**$t_6$  and  $t_7$ :** In step 7, the maximal deceleration ( $-\varepsilon_m$ ) is used. So, it gives  $t_7 - t_6 = t_5 - t_4$ . If  $S_5$ ,  $S_6$ , and  $S_7$  are the areas of steps 5, 6 and 7 on the profile diagram respectively, the following relation holds

$$S_5 + S_6 + S_7 = 2a + w_2(t_3 - t_2) / 2 \quad (18)$$

Using (17), the duration of step 6 is given as

$$t_6 = t_4 + [4a + w_2(t_3 - t_2)] / (2w_0) \quad (19)$$

**Average speed  $\dot{x}_1$ :** The average speed is the position of the capsule shell at  $t_2$  divided by the cycle time. It can be considered as a performance index to compare the proposed approaches. Using (11), the average speed is given as

$$\dot{x}_1 = \left( \frac{2m}{M+m}a - \frac{1}{2}\mu_{1k}gt_2^2 \right) / t_7 \quad (20)$$

Summarizing the above, the parameters of the formula (5) can be computed using (9)-(19). Thus the desired inner mass velocity profile can be found. On the other hand, the trajectories of the desired inner mass position ( $x_{2d}$ ) and the desired acceleration ( $\ddot{x}_{2d}$ ) can be computed using (5).

## 5. CONTROL APPROACHES

### 5.1 OLC approach:

From the discussion above, it is known that the fast motion (steps 1 and 2) and the slow motion (steps 3-7) are included in one full cycle. During the fast motion, the capsule shell moves forward ( $\dot{x}_1 > 0$ ). During the slow motion, the capsule shell is at rest ( $\dot{x}_1 = 0$ ). So, the desired capsule shell velocity can be computed using (3) as below

$$\dot{x}_{1d} = \begin{cases} -[m\ddot{x}_{2d} + \mu_{1k}(M+m)gt] / M & t \in [0, t_2) \\ 0 & t \in [t_2, t_7] \end{cases} \quad (21)$$

Using (5), the desired inner mass acceleration is given as

$$\ddot{x}_{2d} = \begin{cases} -[2\mu_{1k}(M+m)g + \mu_{2k}mg] / m & t \in [0, t_1) \\ (w_1 - w_2) / (t_2 - t_1) & t \in [t_1, t_2) \\ \mu_{1k}(M+m)g / m & t \in [t_2, t_3) \\ 0 & t \in [t_3, t_4) \\ \mu_{1k}(M+m)g / m & t \in [t_4, t_5) \\ 0 & t \in [t_5, t_6) \\ -\mu_{1k}(M+m)g / m & t \in [t_6, t_7] \end{cases} \quad (22)$$

Putting (21), (22) and (5) in (2) gives the desired open-loop control law

$$u_d = -m\ddot{x}_{2d} - \mu_{2k}mg \operatorname{sgn}(\dot{x}_{2d} - \dot{x}_{1d}) \quad (23)$$

### 5.2 CLC approach:

From (2), we have

$$\ddot{x}_2 = -[u + \mu_{2k}mg \operatorname{sgn}(\dot{x}_2 - \dot{x}_1)] / m \quad (24)$$

The control law can be selected, using partial feedback linearization, as

$$u = \alpha\tau_d + \beta \quad (25)$$

where  $\alpha = -m$ ,  $\beta = -\mu_{2k}mg \operatorname{sgn}(\dot{x}_2 - \dot{x}_1)$ . Let  $\tilde{x}_2 = x_2 - x_{2d}$  be the tracking error; choosing  $\tau_d = \ddot{x}_{2d} - k_v \dot{\tilde{x}}_2 - k_p \tilde{x}_2$  and applying control law (25) to (2) gives the error equation as

$$\ddot{\tilde{x}}_2 + k_v \dot{\tilde{x}}_2 + k_p \tilde{x}_2 = 0 \quad (26)$$

The values of  $k_v$  and  $k_p$  can easily be selected to make the inner mass follow the desired trajectory profile.

### 5.3 SSC approach

Due to the difficulties of implementing the OLC and the CLC in real experiments, a simple switch control approach is proposed. The purpose of the SSC is to utilize the control input profile learnt from the OLC and the CLC to solve the control issues in real experiments. The SSC approach is not a trajectory tracking-based method, but it can move the capsbot in a desired direction effectively.

The idea of the SSC is derived from the seven-step motion strategy. Three constant control signals will be alternately applied to the system. The control flow chart is shown in Figure 3.

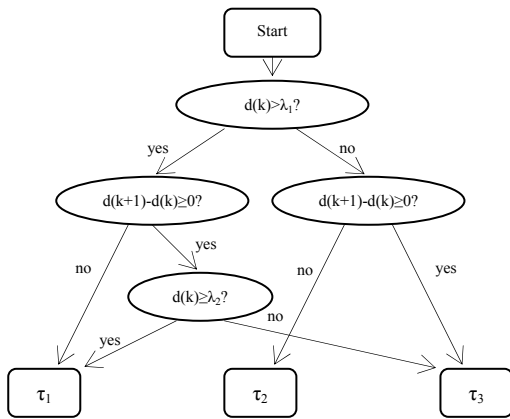


Figure 3 Simple switch control flow chart

where  $k$  is an integer from  $0$  to  $+\infty$ ,  $d(k)$  is the relative mass position at the  $k^{\text{th}}$  sampling interval,  $d(k+1)$  is the relative mass position at the  $(k+1)^{\text{th}}$  sampling interval,  $\lambda$  is the region boundary. The parameters  $\lambda_1$ ,  $\lambda_2$ ,  $\tau_1$ ,  $\tau_2$ , and  $\tau_3$  are decided using the simulation study and will be given in section 6.

## 6. SIMULATION STUDY

### 6.1 Simulation setup

To distinguish the friction coefficient, kinetic and static friction coefficients are used in the system model. In general, the static friction coefficient is about twice the kinetic friction coefficient. Thus the relations  $\mu_{1s}=2\mu_{1k}$  and  $\mu_{2s}=2\mu_{2k}$  are used in the model. The simulation is carried out using MATLAB/SIMULINK with the sampling interval  $T_s=10\text{ms}$ . To avoid collision between the two masses, the following constraint is used in the model

$$-[a + w_2(t_3 - t_2)/2 + e_r] < x_2(t) - x_1(t) < a + e_r \quad (27)$$

where  $e_r$  is the maximal allowable error for the system. If the relative position exceeds the limited region, the simulation

will be terminated. All of the parameters used in the simulation are given in Table 1.

| M (kg)    | m (kg)      | a (cm)      | $\mu_{1s}$ (N/m/s) | $\mu_{2s}$ (N/m/s) | g (m/s <sup>2</sup> ) |
|-----------|-------------|-------------|--------------------|--------------------|-----------------------|
| 0.9       | 0.6         | 30          | 0.166              | 0.016              | 9.81                  |
| $t_1$ (s) | $t_2$ (s)   | $t_3$ (s)   | $t_4$ (s)          | $t_5$ (s)          | $t_6$ (s)             |
| 0.4       | 0.49        | 0.98        | 1.48               | 1.58               | 5.66                  |
| $t_7$ (s) | $w_1$ (m/s) | $w_2$ (m/s) | $w_0$ (m/s)        | $e_r$ (cm)         | $T_s$ (ms)            |
| 5.76      | 1.66        | 1.0         | 0.2                | 5                  | 10                    |

### 6.2 OLC approach

Figure 4 shows the capsbot motion in one full cycle under the OLC law (23).

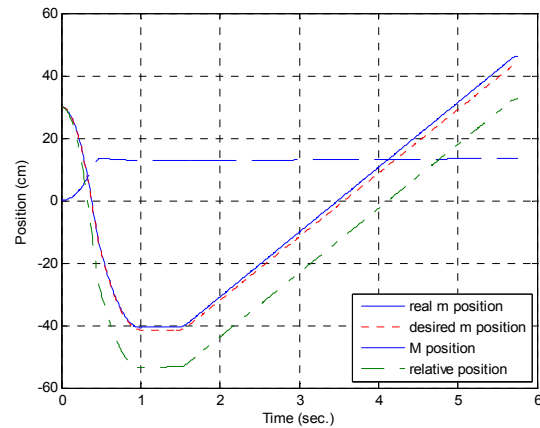


Figure 4 Trajectories of position in one cycle using the OLC

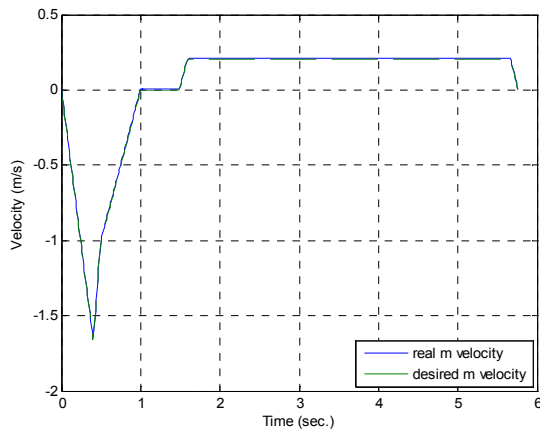


Figure 5 Trajectory of velocity in one cycle using the OLC

From Figure 4, we can see that the desired position profile has not been tracked properly and the capsule shell cannot remain at rest during the slow motion. Figure 5 shows that the desired velocity profile is tracked with errors during the slow motion. The capsbot moves 13.56 cm in 5.8 seconds. The average speed is about 2.34 cm/s. On testing the OLC approach for several cycles, the system terminates at the second cycle where the relative position does not satisfy the constraint (27). This demonstrates that the OLC law makes the system unstable and cannot be implemented.

### 6.3 CLC approach

The CLC approach is implemented using the control law (25). To make the error equation (26) converge faster and restrain noise disturbances, the linear feedback gain is chosen as  $k_p=100$ ,  $k_v=50$ . The simulation results in one full cycle are shown in Figure 6 and Figure 7. The system trajectory in continuous cycles is shown in Figure 8.

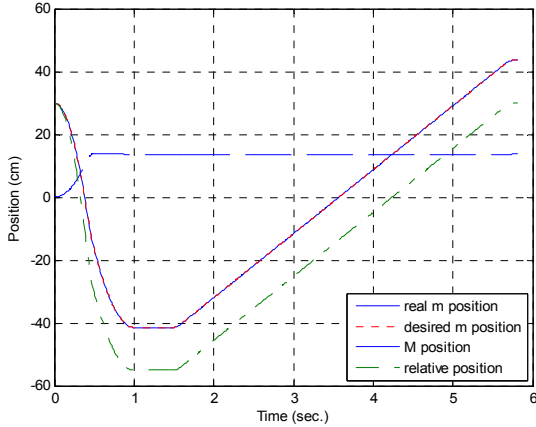


Figure 6 Trajectories of position in one cycle using the CLC

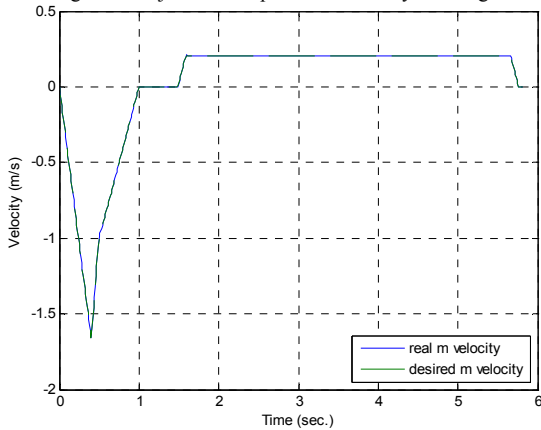


Figure 7 Trajectory of velocity in one cycle using the CLC

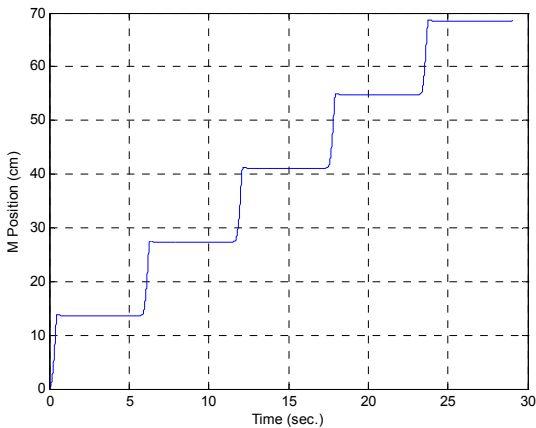


Figure 8 Trajectory of the capsbot in five continuous cycles using the CLC

From Figure 6, we see that the CLC approach gives a much better performance than the OLC approach. The desired position has been tracked properly with little error. The capsule shell is almost at rest during the slow motion. The desired velocity profile is followed with little error as shown in Figure 7. The capsbot moves 13.71 cm in 5.8 seconds.

The average speed is about 2.36 cm/s. Figure 8 gives the system trajectory in five cycles over a period of 29 seconds. It shows that the CLC can effectively reduce tracking errors and makes the system track the desired trajectory properly.

### 6.4 SSC approach

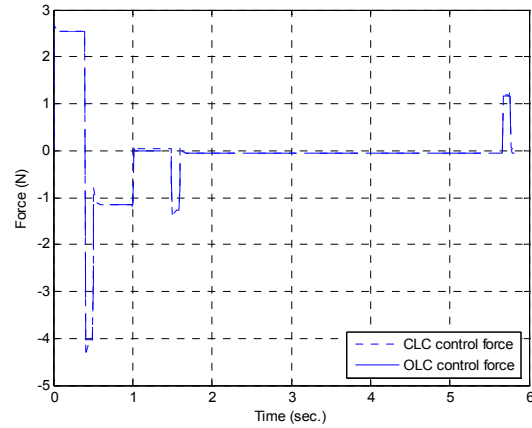


Figure 9 Control forces used in the OLC and the CLC

The selection of control inputs  $\tau_1$ ,  $\tau_2$  and  $\tau_3$  derives from the experience of the OLC and the CLC. Figure 9 above shows the control forces used in the OLC and the CLC. The maximal force in Figure 9 is about 4N, so a smaller accelerated force  $\tau_1=3N$  is tried for the system in the accelerated region. To avoid the backward movement of the capsbot, a decelerated force is selected at  $\tau_2=-1N$ . To drive the capsbot as fast as possible, a sufficiently large accelerated region should be chosen, so the boundaries  $\lambda_1, \lambda_2$  are chosen as 0 and  $2a/3$ , respectively. Following the decelerated force  $\tau_2$ , a small accelerated force  $\tau_3=-0.1N$  is used to move the inner mass  $m$  forward while keeping the shell  $M$  as stationary as possible. To allow comparison with the other two approaches, the trajectory using the SSC is shown in Figure 10.

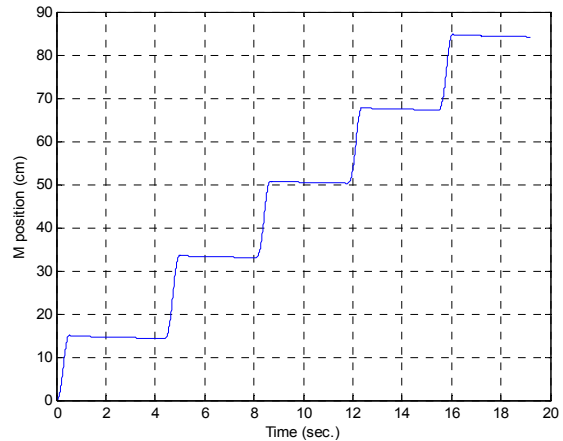


Figure 10 Trajectory of the capsbot in five continuous cycles using the SSC

Figure 10 shows that the capsbot moves 84.1 cm in five cycles and 19.2 seconds, and the average speed of the system is 4.38 cm/s. We can see in the figure that the SSC approach improves its performance after the first cycle. The results therefore show that the SSC has “training” and “learning” abilities, which improve the performance of the controller every cycle.

### 6.5 Comparison

Comparing the three proposed approaches reveals that the CLC gives a better performance in trajectory tracking. The OLC gives an acceptable tracking performance for one single cycle. But the tracking error leads to mass collision after two cycles. Thus the OLC approach can not be implemented in real experiments, in which there is always noise and disturbances. Using the CLC approach allows the desired velocity trajectory to be tracked with little error, but it is more difficult to implement than the SSC. The implementation of the CLC needs four sensors which are

used for measuring position and velocity, while the SSC only needs two sensors for measuring position. Compared with the other two approaches, the SSC gives a faster movement and is more robust to external disturbances. However, the shortcoming of the SSC is that it is difficult to decide upon the position and velocity of the system, which are unpredictable. Furthermore, the SSC energy consumption is high, as the friction during the small backward movement of the capsbot on each cycle consumes a lot of energy. A performance summary of the three approaches studied in this paper is presented in Table 2.

Table 2 Performance summary of proposed approaches

| Approach | Average velocity (cm/s) | Maximal force (N) | Complexity | Tracking performance | Robustness | Energy consumption |
|----------|-------------------------|-------------------|------------|----------------------|------------|--------------------|
| OLC      | 2.34                    | 4.03              | No         | Unstable             | Bad        | Inefficient        |
| CLC      | 2.36                    | 4.37              | Yes        | Good                 | Good       | Efficient          |
| SSC      | 4.38                    | 3                 | No         | Poor                 | Good       | Inefficient        |

## 7. CONCLUSIONS

This paper has studied the tracking issue of the capsbot has from the viewpoint of the underactuated dynamic system. An optimal seven-step motion strategy has been proposed. A trajectory profile based on the proposed strategy has been generated. Three control approaches have been investigated: the open-loop control law, the closed-loop control law using partial feedback linearization, and the simple switch control law. The simulation results have been presented to demonstrate the proposed approaches. A brief comparison of the proposed approaches has also been made.

The implementation of a lab-based rig is under development. This device consists of three parts: a capsule shell, a piezoelectric element, and an inner mass. An optical encoder is used on the device to measure the position of the capsbot at real time. This system can be used by researchers as a test bed to demonstrate the proposed approach. Further work in this research area will include robust control with parameter uncertainty, iterative learning control using repetitive continuous cycles, and test of the device in a real complicated environment.

**Acknowledgements:** The authors would like to thank the EPSRC research council (research grant EP/E025250/1) and Dr. Price Emma for their support of this research.

### REFERENCES

Chernousko, F. L. (2002): "The Optimum Rectilinear Motion of a Two-mass System." In *Journal of applied Mathematics and Mechanics*, **53**, pp. 1-7.

Li, H., K. Furuta, and F. L. Chernousko (2005): "A Pendulum-driven Cart via Internal Force and Static Friction." In *Proc. of Conference on Physics and Control*, pp. 15-17. St. Petersburg, Russia.

Li, H., K. Furuta, and F. L. Chernousko (2006): "Motion Generation of the Capsbot using Internal Force and Static Friction." In *Proc. of the 45<sup>th</sup> IEEE Conference on Decision and Control*, pp. 6575-6580, San Diego, USA.

Liu, Y., H. Yu, and B. Burrows (2007): "Optimization and Control of a Pendulum-driven Cart-pole System." In *Proc. of the 2007 IEEE International Conference on Networking, Sensing and Control*, pp. 151-156. London, UK.

Karagozler, M. E., E. Cheung, K. Jiwoon, and M. Sitti (2006): "Miniature Endoscopic Capsule Robot using Biomimetic Micro-Patterned Adhesives." In *Proc. of the 1<sup>st</sup> IEEE/RAS-EMBS International Conference on Biomedical Robotics and Biomechanics*, pp. 105-111.

Kim, B., S. Park, C. Y. Jee, and S. J. Yoon (2005): "An Earthworm-like Locomotive Mechanism for Capsule Endoscopes." In *Proc. of IEEE/RSJ International Conference on Intelligent Robots and Systems*, pp. 2997-3002.

Kosa, G., M. Shoham, and M. Zaaroor (2005): "Propulsion of a Swimming Micro Medical Robot." In *Proc. of the 2005 IEEE International Conference on Robotics and Automation*, pp. 1327-1331. Barcelona, Spain.

Stefanini, C., A. Menciassi, and P. Dario (2006): "Modeling and Experiments on a Legged Microrobot Locomoting in a Tubular, Compliant and Slippery Environment." *International Journal of Robotics Research*, **25**, pp. 551-560.

Yamagata, Y., and T. Higuchi (1995): "A Micropositioning Device for Precision Automatic Assembly using Impact Force of Piezoelectric Elements." In *Proc. of the IEEE International Conference on Robotics and Automation*, pp. 666-671.

Yu, H., Y. Liu, T. C. Yang (2007): "Tracking Control of a Pendulum-driven Cart-pole Underactuated System." In *Proc. of the 2007 IEEE International Conference on Systems, Man and Cybernetics*, Montreal, Canada.